1. Omokhafe James TOLA[1], 2. Emeka Simon OBE[2], 3. Chinedu Titus OBE[2], 4. Linus Uchechukwu ANIH[2]

Electrical and Electronic Department, Federal University of Technology Minna , (1), Electrical Department, University of Nigeria Nsukka (2)
ORCID. 1. 0000-0003-2134-063X, 2. 0000-0001-9530-2009, 3. 0000-0002-8553-8859, 4. 0000-0002-5202-8940

doi:10.15199/48.2022.04.11

Finite Element Analysis of Dual Stator Winding Line Start Permanent Magnet Synchronous Motor

Abstract*. This paper presents the analysis of dual stator winding line-start permanent magnet synchronous motor (PMSM) developed using finite element analysis (FEA) software suitable for comparison to the conventional line-start PMSM. A three-phase, 4 poles, 36 slots double layer interior permanent magnet (IPM) motor was characterised and its winding structure reconfigured into the dual stator winding with the same capacity and power rating as the conventional motor. The starting, synchronisation capability and the developed torque were compared. The results showed that the DSWPMSM synchronised at 0.20s and operated on a steady speed of 1500rpm.*

Streszczenie. *W artykule przedstawiono analizę silnika synchronicznego z magnesami trwałymi (PMSM) z podwójnym uzwojeniem uzwojenia, opracowanego przy użyciu oprogramowania do analizy elementów skończonych (FEA), odpowiednią do porównania z konwencjonalnym PMSM o rozruchu liniowym. Scharakteryzowano trójfazowy, 4 biegunowy, 36 żłobkowy dwuwarstwowy silnik z wewnętrznym magnesem trwałym (IPM) i przekonfigurowano jego strukturę uzwojenia na uzwojenie z podwójnym stojanem o tej samej pojemności i mocy znamionowej, co silnik konwencjonalny. Porównano zdolność rozruchową, synchronizacyjną i opracowany moment obrotowy. Wyniki pokazały, że DSWPMSM synchronizował się w 0,20 s i działał ze stałą prędkością 1500 obr./min.* (***Analiza metodą elementów skończonych podwójnego uzwojenia stojana silnika synchronicznego z magnesami trwałymi***)

Keywords: Finite element analysis; Dual stator winding; Line-start PMSM; Steady speed; Developed Torque.
Słowa kluczowe: uzwojenie stojana, silnik synchroniczny, metoda elementów skończonych.

Introduction

Much attention has been given to research on permanent magnet synchronous motor (PMSM) due to high technological design and advances in permanent magnet materials. PMSM become an attractive alternative to induction motors in several applications due to its comparatively higher efficiency, power factor, power density and a superior heat transfer capability [1],[2]. Its efficiency is superior to those obtained with asynchronous motors, while its cost of production is higher.

The new standard, IEC/EN60034-30:2008, of motor efficiency plays an important role in reducing the amount of energy used by motors. This standard introduces five new IE (International Efficiency) classes- IE1 (standard efficiency), IE2 (high efficiency), IE3 (premium efficiency), IE4 (super premium efficiency) and IE5 (ultra-premium efficiency) [3]. In order to reach the high efficiency, IE4 and IE5 are essential to motor design industries.

The line-start PMSM is a hybrid motor which has the ability to start by direct on connection to a power supply without the use of power electronic converters. Moreover, it is a combination of high energy permanent magnet and a cage rotor, described in two starting modes: asynchronous and synchronous. The motor possesses a higher power factor and efficiency compared to the induction motor of the same rating [4].

Synchronous motors and induction motors are widely used in the industries as the most common drive due to their robustness and simplicity during construction. The needs for new types of motors in the industrial applications has grown over the last few years as a result of high demand inaccuracy, high torque and high efficiency in the dynamic performance. Line-start PMSM has gained interest due to high efficiency, high torque, high power density and robustness.

Over the last few years, researchers have focused on research on multiphase PMSM with different methods proposed on the performance characteristics compared to the conventional three-phase PMSM. The machine is known for fault tolerance capability, improve reliability and employed to reduce the most harmful mmf space harmonics [5], [6]. Despite the merits, the machine suffers from an immoderate heat dissipation in the winding, a large amount of power is drawn to start, and the machine operates stunted lagging power factor.

In the literature, several researchers also focused on improving on the performance of induction and reluctance motors using dual stator winding [7]–[11]. In [12]–[14], improving the performance of electrical machines with two stator winding and connected with a balanced capacitor were described. However, there few studies in the literature in the field of dual stator winding PMSM. In [15], the author demonstrated the capabilities of a multiphase PMSM and compared with the conventional three-phase PMSM.

DSWPMS has high torque, high efficiency and power density because the motor utilises the magnetic and reluctance torque. In order to verify the effectiveness and performance, the motor design is validated by simulation on finite element software ANSYS Electromagnetic suite.

In this paper, the effects of the dual stator winding on the dynamics performance of the motor using FEM software is studied in order to enhance the output torque of the motor. The torque quality is essential to the motor performance. The main and auxiliary windings have a direct effect on the electromagnetic and torque with the appropriate capacitor value. The design-maintained squirrel cage bar, and permanent magnet (PM) in the rotor while the stator winding is reconfigured to accommodate the two sets of windings. The stator consists of 36 slots, and the windings are curly in a double layer with q=3 slot per pole per phase.

The main contribution of this work is the finite element analysis of DSWPMSM with capacitor current injection using ANSYS electromagnetic suite was investigated in order to study the effect on the motor, the electromagnetic torque, rotor speed with load, stator winding currents and induced voltage. The simulation results have provided valuable information for the realisation of the model.

Phase variable Model of Dual stator winding PMSM

The mathematical model need for the modeling of DSWPMSM is worked out in phase stationary variables that represent stator voltage, inductance and flux linkages of permanent magnet sets [16] are derived as:

$$(1)\quad \begin{cases} V_{ABCs} = R_{ABC} i_{ABCs} + \dfrac{d\lambda_{ABCs}}{dt} \\ 0 = R_{XYZ} i_{XYZs} + \dfrac{d\lambda_{XYZs}}{dt} + Vc_{XYZs} \\ V_{dqr} = R_{dqr} i_{dqr} + \dfrac{d\lambda_{dqr}}{dt} \end{cases}$$

The stator and rotor variables are described by subscript *s* and *r* respectively while the main and auxiliary windings are also described by ABC and XYZ respectively. The ABC and XYZ winding resistance per- phase are R_{ABC} and R_{XYZ} respectively. The flux linkages expression is presented as.

$$(2)\quad \begin{cases} \lambda_{ABCs} = L_{ABC} i_{ABCs} + L_{ABCXYZ} i_{XYZs} + L_{\cdot 1r} i_{\cdot dq} + \lambda_{(PM)} \\ \lambda_{XYZs} = L^{T}_{ABCXYZ} i_{ABCs} + L_{XYZ} i_{XYZs} + L_{\cdot 2r} i_{\cdot dq} + \lambda_{(PM)} \\ \lambda_{\cdot dqr} = L^{T}_{\cdot 1r} i_{ABCs} + L^{T}_{\cdot 2r} i_{XYZs} + L_{\cdot r} i_{\cdot dqr} + \lambda_{(PM)} \end{cases}$$

The inductances are represented in matrix form as:

$$(3)\quad L_{SS} = \begin{bmatrix} L_{ABC} & L_{ABCXYZ} & L_{1r} \\ L_{ABCXYZ} & L_{XYZ} & L_{2r} \\ L_{1r} & L_{2r} & L_r \end{bmatrix}$$

$L_{ABCXYZ}=L_{12}+L_{l12}$

where L_{12} is the mutual inductances between the two winding and L_{l12} is the mutual leakage inductances between the two winding, $\lambda_{(PM)}$ is the PM material flux, and it linked to the stator and the two-rotor damper. Because of sinusoidal distribution flux linkages, the PM flux linkages are defined as.

$$(4)\quad \lambda_{(PM)} = \begin{bmatrix} \lambda_{pmrq} \\ \lambda_{pmrd} \end{bmatrix} = \begin{bmatrix} \lambda_m \cos\theta_r \\ \lambda_m \sin\theta_r \end{bmatrix}$$

The Finite Element Method

During the pas years, the approximate magnetic field inside electrical machines is mostly calculated using a magnetic circuit which requires the assumption of the magnetic flux paths as a significant limitation of the method [17], [18]. However, the finite element method (FEM) deal with the complex rotor structure of an electrical machines for more accurate calculation [19]. FEM is a powerful numerical method used to ascertain correctly the effects of the machine geometric, saturation effects and other variables associated with the magnetic field.

FEM can be obtainable in the form of computer software called ANSYS Electromagnetic suite (MAXWELL 2018). This requires no assumption of the magnetic flux paths. The ANSYS cleave the magnetic field thereby set aside a scalar potential at every node for a comparable solution of magnetic field intensity H. And to get an exact kind of the field, each element of the model is compact for the field to be suitably interpolated from the nodal values. The precision of the solution turn on how small each of the discrete element is. However, there is a concession between the number of elements and the number of computing resources need for the computation.

During the last decades, FEM has become the prefered tool for design and computation of the parameters of electrical machine. The FEM has an advantage where the machine design details and the materials used are well defined.

FEM is a dedicated technique used to analyse the electromagnetic field or thermal analysis. This become popular owing to the recent development in the processing speed of computers.

Recently, there are commercial FEM programs available and used to determine the different type of electrical parameters and material saturation in a different part of the machine. In this paper, the ANSYS electromagnetic suite is used which allow both steady-state and transient analysis.

Two-dimensional (2D) and three-dimensional (3D) are the most popular solver in FEM. However, 2D FEM is the most commonly used in 2D than 3D, and permanent magnet synchronous motor has a typical factor that requires a 2D calculation to achieve accurate results. The magnet edges are often appropriately shaped concerning the stator slots in order to reduce the cogging effect. This means that PMSMs practically require 2D calculation.

The process modeling and calculation in a single stage of FEA may take days or even a week which is far too slow most, especially if it requires more iterations in the process. However, with the developments in technology and high computer configuration in recent years, it makes the modeling and calculation faster and more accurate.

The FEM is found on energy conversion of electric machines obtained from Maxwell equations can be shown as [20] :

$$(5)\quad -\int_v \bar{E}.\bar{J}dV = \int \bar{H}.\frac{\partial \bar{B}}{\partial t}dV$$

where B is the magnetic flux density, H is the field intensity, J is the current density, E is the electric field, and V is the volume enclosing the analysed machine.

The electrical power input is the left-hand side which can be shown as:

$$(6)\quad -\int_v \bar{E}.\bar{J}dV = \frac{\partial}{\partial t}\int_v \left(\int_0^B \bar{H}.d\bar{B} \right) dV$$

Moreover, the rate of increase of the stored magnetic energy is the right-hand side is expressed as:

$$(7)\quad W_m = \int_v \left(\int_0^B \bar{H}.d\bar{B} \right) dV$$

It is well known that the curl of magnetic vector potential A is equal to the magnetic flux density B, while the divergence is equal to zero. Therefore the expression shown the input power expressed as a magnetic vector potential is given as:

$$(8)\quad \bar{B} = \bar{\nabla} \mathrm{X} A$$

By Faraday's law,

$$(9)\quad \bar{\nabla} \mathrm{X} \bar{E} = -\frac{\partial \bar{B}}{\partial t}$$

Hence,

$$(10)\quad \bar{\nabla} \mathrm{X} \bar{E} = \frac{\partial}{\partial t}\left(\bar{\nabla} \mathrm{X} \bar{A} \right)$$

Electrostatic potential can be neglected if there is no power loss. If the electric scalar potential denoted by φ the then electric field can be expressed as

(11) $$\bar{E} = \frac{-\partial \bar{A}}{\partial t} - \nabla \phi$$

Using Ampere's law and magnetic vector potential, the governing equation can be expressed as

(12) $$J = \nabla X \left(\frac{1}{\mu} \nabla X A \right)$$

If the axial core length is l and the voltage between the ends of the conductor is u, the electric scalar potential in the axial direction (z) in the conductor can be expressed as

(13) $$\phi = -\frac{u}{l} z$$

Then the effects of the eddy current density present in the conducting medium are expressed as

(14) $$J_e = -\sigma \frac{\partial A}{\partial t} - \frac{\sigma}{l} u$$

The effect of the high energy of the PM infused in the cage rotor is represented as J_m.

Consequently, the sum of the current density in the entire core is expressed as [4].

(15) $$J = J_e + J_m$$

It should be noted that the reluctance torque is produced by the interaction of ABC and XYZ winding and the torque self-start the motor. The torque developed owing to the permanent magnets when current induced in the stator windings produce a braking torque that may prevent the motor from reaching synchronous speed. The third torque is developed as a result of the interaction between the dual stator windings, and rotor cage winding is the major torque available at motor transients. The afore-mentioned torques are the overall torque the proposed motor.

Therefore the motor output torque can be obtained by the expression in (16)

(16) $$T_{out} = \frac{\partial}{\partial \theta} \int_v \int_0^H \bar{B} dH dV$$

Where θ is the angular displacement

The triangular mesh used for entire model mesh is of stator laminations, rotor laminations and the air-gap the generated mesh for the formulation of finite element problem. The area to analyse is subdivided into triangles, or quadrilaterals call finite elements. Each of these has three vertices call grid point (in case of triangles). Given the motor geometry, this mesh can be generated automatically in the software for the best solution accuracy.

The Finite Element Model of PMSM

The proposed machine is characterised using the parameter of a known machine. In this study, the geometry of the machine was set based on the parameters in [21] as given in *Table 1*. While setting the machine model, it is deemed necessary to find out the physical and electrical parameters to model it accurately. The equivalent circuit of the motor was built and transformed into Maxwell geometry to give a circular 2-D machine as presented in Fig. 1 as an FEA model in ANSYS Maxwell. The FEA model utilised a non-linear material in rotor and stator to offer high saturation flux density and relatively good permeability. Conventionally, selected non-linear material is M19-24G steel as shown in *Table 1*. where M19-24G is a class of Silicon steel material with a core loss of 19 W and 24 Gauge by the standard.

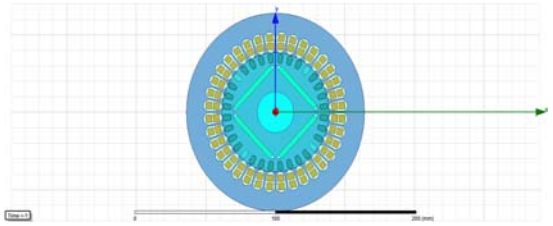

Fig. 1: 2-D Geometrical section of the model machine

Table 1: FEA Machine parameters

Parameters	Value
Rated power	4 HP
Phase voltage	230
Rotational speed	1500 rpm
Winding layout	Double layer
Steel Type	M19_24G
Permanent Magnet	Nd-Fe-B
Poles	4
Stack length	70 mm
Number of slots	36
Number of turns	56
Core length	70 mm
Stator outer diameter	128 mm
Stator inner diameter	77 mm
Rotor outer Diameter	76.2 mm
Rotor inner Diameter	26 mm

The stator of the proposed machine is built by dividing the original three-phase winding into two separate three-phase windings wound on a similar pole. Moreover, a full pitched, double layer winding is developed for this research work. The clock diagram showing the stator winding is 36 slots, four poles, three-phase full pitched coils are presented in *Fig.* 2. The main winding ABC and the auxiliary winding XYZ alternate between the double layer. Where a^- is the coil carrying current out of the paper from phase a, and b^+ is the coil carrying current into the paper from phase b.

Since the number of slots per pole per phase is an integer, an integral slot winding is possible. Therefore, an integer slot winding is used in the design of the stator coil configuration.

The stator winding was modelled based on information in *Fig.* 2. The auxiliary windings XYZ were changed to external to enable the FEA model couple with a capacitor in the external circuit, and the mechanical load was applied via the Simplorer mechanical load source.

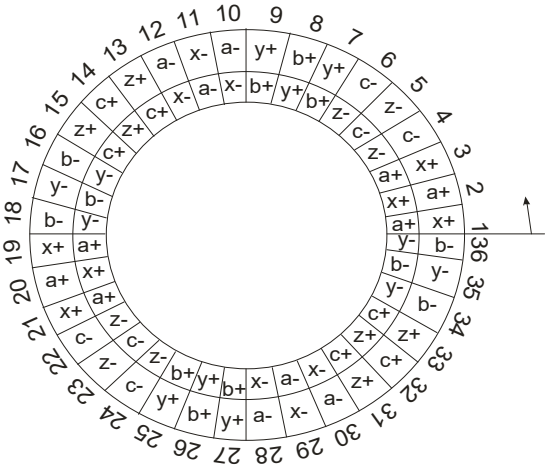

Fig. 2: Clock diagram of full pitched distributed stator winding

FEA Model and Simplorer Co-simulation.

The inability of Maxwell FEA to have allowed connection of capacitor across the auxiliary winding is a significant limitation. To overcome this limitation, the Maxwell FEA model is coupled to Simplorer and simulation is performed by Co-simulation in order to verify the performance as shown in *Fig. 3*, which consists of the FEA Model motor, the mechanical system (Load torque and speed source) and the coupled capacitors via resistance and inductance. Furthermore, at 0.5s, a load torque of 18.9713Nm is applied to the machine.

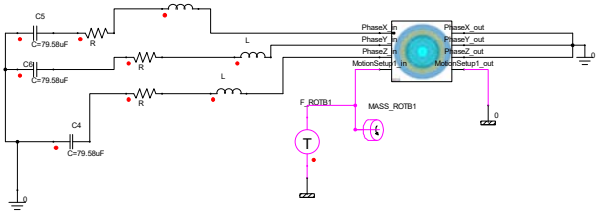

Fig. 3: The Coupling of FEA Model with Simplorer

Simulation Results and Discussion

The field solution of the geometry is obtained by running the solution setup in ANSYS Maxwell to solve all the important Maxwell's equations and its called processing. Once the processing is completed, all the important plots are obtained.

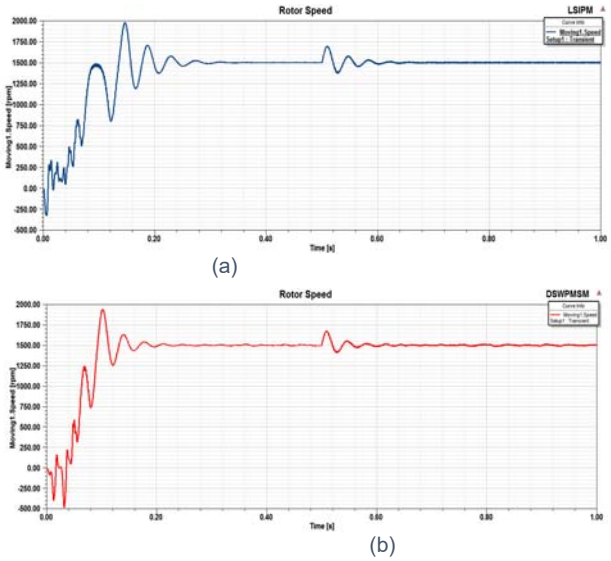

Fig. 4: FEA Speed Characteristics during synchronization (a) Conventional motor (b) DSWPMSM

The starting characteristics of the motors and the time to reach the synchronous speed was observed. *Fig. 4* gives the plot of the rotor speed versus time of Line start IPM and DSWPMSM, respectively. The simulation was carried out for 1s at a step time of 0.00005s. The starting performance was equally carried out with the rated load torque. It can be observed that the motor synchronised at 0.20s and operate on a steady speed of 1500 rpm. However, the conventional IPM got synchronised at 0.32s of the 1500rpm. In term of starting characteristic, the model machine is better than the conventional machine.

The electromagnetic torque of the machines in *Fig. 5*. The average torque becomes zero as soon as the machine reached the synchronous speed as shown. Both machines have a high starting torque.

Fig. 6 shows the phase current of the proposed machine. The operation of the motor from the mains supply is attractive since the current taken from both the main and auxiliary are relatively low. Moreover, a low current transmutes to reduce losses, which will finally lead to high efficiency.

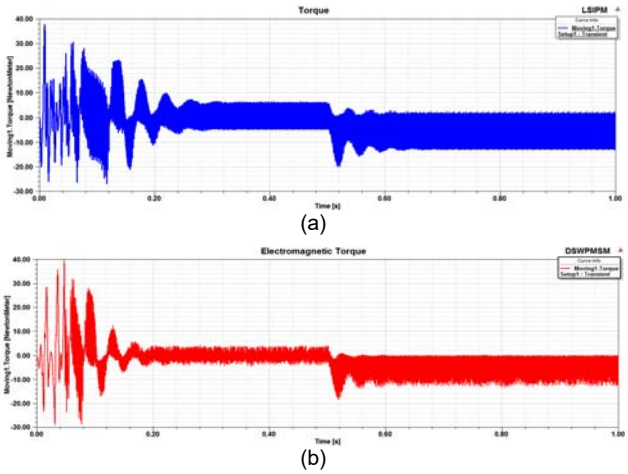

Fig. 5: FEA of Torque Characteristics (a) conventional motor (b) DSWPMSM

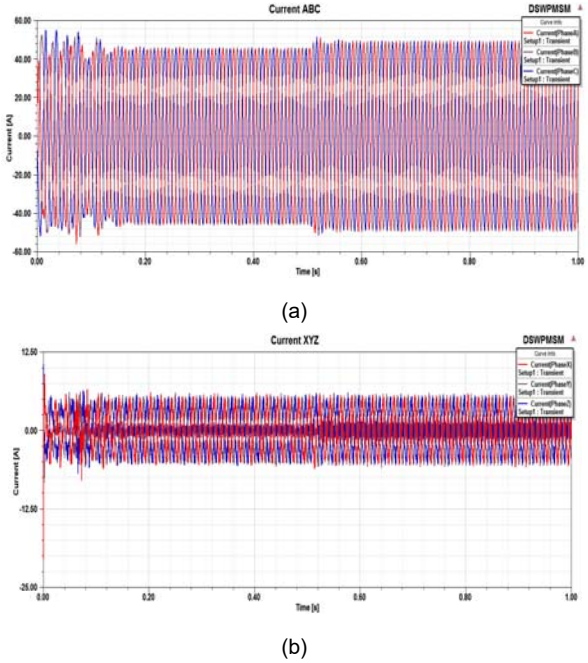

Fig. 6: FEA Phase Current Characteristics of DSWPMSM (a) Main winding (b) Auxiliary winding

The motor performance can be observed by study the magnetic field distribution. The magnetic field distribution over the entire geometry in the conventional and the proposed machine is presented with a different colour that shows the level of saturation in the areas. From the results in Fig. 7, it shows that the magnetic flux density is high in the core part of the motor because the steel is highly saturated close to the magnet. However, the saturations appeared because of the magnet strength. The orange and green areas represent the higher flux density, and the blue areas represent lower flux density in the motor. Fig. 7 shows the magnetic flux density of the Line start IPM and DSWPMSM, respectively. The interaction magnetic field between them can clearly show the stator windings, cage windings and the magnetic field produced by the PMs. The results show that the magnitude of the flux density in the model machine is higher than the one in the conventional machine. As presented in Fig. 8, the flux linkages are

sinusoidal with small fluctuation noted at the start-up. However, the starting response of the flux linkage does not affect the performance of the machine.

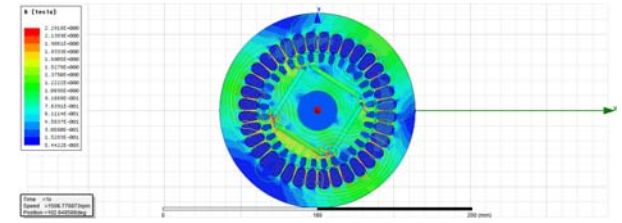

(a)

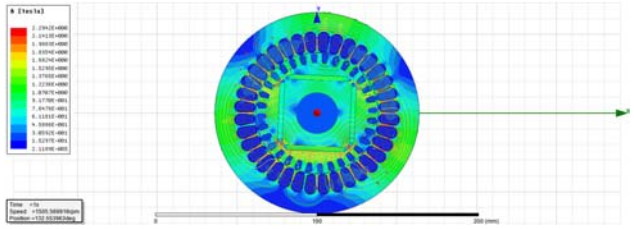

(b)

Fig. 7: Magnetic flux density (a) conventional motor (b) DSWPMSM

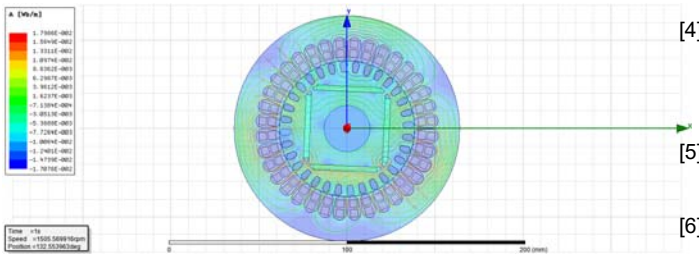

Fig. 8: Magnetic flux line of DSWPMSM

The failure of the capacitor was not discussed in this study. However, the capacitor connected to the auxiliary winding may affect the reliability of the proposed machine. However, this and the price of the capacitor and the auxiliary coils as additional cost compared to the conventional machine. However, the cost can be overlooked by considering the torque enhancement and the good power factor of the model machine.

Conclusion

In this paper, a dynamic model 2D FEM in Ansys Maxwell software is presented to compute the performance of a dual stator winding line start interior PMSM with capacitor current injection.

The finite element analysis of the conventional line start IPM, and the DSWPMSM had been developed with the same dimension and rotor structure. The auxiliary winding was equipped with capacitance current injection and co-simulated by coupling the FEA model and capacitor in Simplorer. It is observed from the starting characteristics that the motor is capable of starting. The magnetic flux density and flux lines were determined for both conventional and model machine.

Validation of the transient dynamic and transient of the model with FEA software ANSYS Electromagnetics suite has been realised.The speed and torque obtained from the co-simulation were compared to the results of Line Start IPM. Pulsations were observed, in the FEA models during starting, which is caused due to the geometry of the machine.

***Authors**: Dr. Omokhafe James Tola, Dept. of Electrical & Electronics Engineering, Federal University of Technology, Minna, Nigeria. E-mail: omokhafe@gmail.com*
Prof. Emeka Simon Obe, Dept. of Electrical Engineering, University of Nigeria, Nsukka, Nigeria. E-mail: simon.obe@unn.edu.ng
Eng. Chinedu Titus Obe, Dept. of Electrical Engineering, University of Nigeria, Nsukka, Nigeria. E-mail: chinedu.obe@unn.edu.ng (corresponding author)
Prof. Linus Uchechukwu Anih, Dept. of Electrical Engineering, University of Nigeria, Nsukka, Nigeria. E-mail: linus.anih@unn.edu.ng.

REFERENCES

[1] L. Li, J. Zhang, C. Zhang, and J. Yu, “Research on Electromagnetic and Thermal Issue of High-Efficiency and High-Power-Density Outer-Rotor Motor,” *IEEE Trans. Appl. Supercond.*, vol. 26, no. 4, 2016, doi: 10.1109/TASC.2016.2542192.

[2] R. T. Ugale and B. N. Chaudhari, “Rotor Configurations for Improved Starting and Synchronous Performance of Line Start Permanent Magnet Synchronous Motor,” *IEEE Trans. Ind. Electron.*, vol. 64, no. 1, pp. 138–148, 2017, doi: 10.1109/TIE.2016.2606587.

[3] Aníbal T. de Almeida ; Fernando J. T. E. Ferreira ; Ge Baoming, “Beyond induction motors — Technology trends to move up efficiency,” in *49th IEEE/IAS Industrial & Commercial Power Systems Technical Conference*, doi: 10.1109/ICPS.2013.6547330.

[4] Milad Niaz Azari; Mojtaba Mirsalim, “Performance Analysis of a Line-start Permanent Magnet Motor with Slots on Solid Rotor Using Finite-element Method,” *Electr. Power Components Syst.*, vol. 41, pp. 1159–1172, 2013, doi: 10.1080/15325008.2013.809819.

[5] M. F. Barcaro M, Bianchi N, “Analysis and tests of a dual three-phase 12-slot 10-pole permanent-magnet motor,” *IEEE Trans. Industry Appl.*, vol. 46, no. 6, pp. 2355–2362, 2010.

[6] R. Bojoi ; A. Cavagnino ; S. A. Odhano ; A. Tenconi ; S. Vaschetto, “Experimental fault assessment on multiphase PM generators with fractional-slot concentrated windings,” in *IECON 2015 - 41st Annual Conference of the IEEE Industrial Electronics Society*, doi: 10.1109/IECON.2015.7392875.

[7] Mohamed Arbi Khlifi, “Advances and Steady-State Development of Dual Stator-Winding Induction Machine,” *IETE J. Res.*, 2020, doi: 10.1080/03772063.2020.1733443.

[8] P. Junkyu, B. ; Claudio, B. ; Alberto, D. ; Matteo, and N. Bianchi, “Experiment-Based Performance Analysis for Dual Three-Phase Synchronous Reluctance Motor According to Different Winding Configurations,” in *2020 International Symposium on Power Electronics, Electrical Drives, Automation and Motion (SPEEDAM)*, doi: 10.1109/SPEEDAM48782.2020.9161887.

[9] M. Ayaz Khoshhava ; Hossein Abootorabi ; G. R. Arab Markadeh, “Iron Loss Modeling in Dual Stator Winding Induction Machines with Unequal Pole Pairs and Squirrel Cage Rotor,” *IEEE Trans. Ind. Electron.*, pp. 1–1, doi: 10.1109/TIE.2020.2977545,.

[10] D. D. G. . B. Anagha Soman, Dr. Rajesh Holmukhe, “Multispeed Operation and Testing Of Dual Stator Winding Induction Machine,” *Int. J. Sci. Technol. Res.*, vol. 9, no. 1.

[11] R. Ç. Ahmet GÜNDOĞDU, “Performance Analysis of Open Loop V/f Control Technique for Six-Phase Induction Motor Fed By A Multiphase Inverter,” *Turkish J. Sci. Technol.*, vol. 15, no. 2, pp. 111–125, 2020.

[12] L. U. Anih and E. S. Obe, “Performance analysis of a composite dual-winding reluctance machine,” *Energy Convers. Manag.*, vol. 50, pp. 3056–3062, 2009.

[13] E. S. Obe, “Steady-state performance of a line-start synchronous reluctance motor with capacitive assistance,” *Electr. Power Syst. Res.*, vol. 80, no. 10, pp. 1240–1246, Oct. 2010, doi: 10.1016/j.epsr.2010.04.004.

[14] L. U. Anih, E. S. Obe, and S. E. Abonyi, “Modelling and performance of a hybrid synchronous reluctance machine with adjustable X d / X q ratio,” *IET Electr. Power Appl.*, pp. 171–182, 2015, doi: 10.1049/iet-epa.2014.0149.

[15] Gurakuq Dajaku, “Advanced multi phase fractional slot concentrated windings: characteristics and potentials,” *Electr. Eng. Springer*, 2020, doi: 10.1007/s00202-020-01088-2.
[16] O. J. Tola, E. S. Obe, and L. U. Anih, “Modeling and analysis of dual stator windings permanent magnet synchronous motor,” in *IEEE 3rd International Conference on Electro-Technology for National Development (NIGERCON)*, 2017, pp. 861–871, doi: 10.1109/NIGERCON.2017.8281954.
[17] L. Li, N.; Zhu, J.; Lin, M.; Yang, G.; Kong, Y.; Hau, “Analysis of Axial Field Flux-Switching Memory Machines Based on 3-D Magnetic Equivalent Circuit Network Considering Magnetic Hysteresis,” *IEEE Trans. Magn.*, vol. 55, no. 7203104, 2019.
[18] K.-S. Lee, J.-J.; Lee, J.; Kim, “Design of a WFSM for an Electric Vehicle Based on a Nonlinear Magnetic Equivalent Circuit,” *IEEE Trans. Appl. Supercond.*, vol. 28, no. 5206304, 2018.
[19] J.-H. Lee, B.-H.; Hong, J.-P.; Lee, “Optimum Design Criteria for Maximum Torque and Efficiency of a Line-Start Permanent-Magnet Motor Using Response Surface Methodology and Finite Element Method.,” *IEEE Trans. Magn.*, vol. 48, pp. 863–866, 2012.
[20] K. N. & S. Vimalakeerthy, D, “Novel Design of Permanent Magnet Synchronous Reluctance Motor using Finite Element Method,” *Int. J. Eng. Sci. Innov. Technol.*, vol. 2, no. 1, pp. 37–45.
[21] K. Kurihara and M. A. Rahman, “High-Efficiency Line-Start Interior Permanent-Magnet Synchronous Motors”, *IEEE Transactions on Industry Applications,* vol. 40, no. 3, pp. 789–796, 2004.